-RESEARCH PAPER

International Journal of Mining and Geo-Engineering

IJMGE

IJMGE 60-2 (2026) 123-130

DOI: 10.22059/IJMGE.2026.409947.595357

Assessment of potentially toxic elements (PTEs) in kaolin dust and associated human health risks near mining areas in eastern Iran

Ali Najmeddin [a, *], Gholam Reza Lashkaripour [b] and Zohre Boskabadi [b]

[a] *School of Mining Engineering, College of Engineering, University of Tehran, Tehran, Iran.*

[b] *Department of Geology, College of Sciences, Ferdowsi University of Mashhad, Mashhad, Iran.*

Article History:

Received: 24 September 2025.

Revised: 28 November 2025.

Accepted: 31 December 2025.

ABSTRACT

Following reports of silicosis outbreaks among refractory industry workers in eastern Iran, this study analyzed the chemical composition and mineralogical characteristics of mining-derived dust in Ghaenat city and its potential environmental impacts. This study was aimed to investigate the potentially toxic elements (PTEs) concentrations in mine dust and evaluate the human health risk assessment and health effects near mining areas. To achieve this goal, a series of instrumental analyses including XRD, XRF, and ICP-OES have been performed on dust particles. For the better risk assessment, the oral bioaccessibility of PTEs using a simple bioaccessibility extraction test (SBET) was also investigated. X-ray diffraction analysis of dust samples shows that quartz, kaolinite, pyrophyllite, and illite are more abundant, indicating the prevalence of silicates in the dust particles. Calculation of geoaccumulation index indicated that the median Igeo values decreased in the following order: As > S > Sr >> Al ≈ Li ≈ La ≈ Nd ≈ Cu ≈ Pb ≈ Fe ≈ Mg ≈ Zn. Bioaccessibility results revealed pronounced inter-element variability, with arsenic showing the highest bioaccessible fraction (up to 73.1%), particularly in samples collected from the mining area. Although all calculated hazard indices were below the accepted safety threshold, arsenic emerged as the primary contributor to potential health risk.

Keywords: *Mine dust, Health effects, Pollution, Potentially toxic elements, Mineralogy.*

1. Introduction

Mine dust contamination refers to the release of particulate matters (PMs) into the air from mining operations, which can negatively impact both the environment and human health [1]. This contamination is primarily caused by excavation, ore blasting, mineral processing and the movement of materials during mining activities [2]. Elemental pollution in mine dust is a serious environmental and health concern [3]. Mining activities, including the extraction and processing of ores, release dust containing elevated levels of potentially toxic elements (PTEs) into the atmosphere [2]. This dust can contaminate surrounding areas, impacting soil, water, and air quality, and posing risks to both human and ecological health. Airborne dust particles, including those containing PTEs, can travel long distances and contribute to air pollution in nearby urban and rural areas [4]. Inhalation of mine dust can cause various respiratory problems, including bronchitis, asthma, and lung cancer [1]. Exposure to PTEs in mine dust can also lead to cardiovascular diseases, nervous system problems, and reproductive issues [3]. Coal dust and silica dust are two important groups of mine dusts in environmental studies. Occupational exposures to respirable crystalline silica occur in a variety of mines and industries because of its extremely common natural occurrence [5]. Workers with high exposure to crystalline silica include miners, sandblasters, tunnel builders, silica millers, quarry workers, foundry workers, and ceramics and glass workers [2]. Silica refers to the chemical compound silicon dioxide (SiO_2), which occurs in a crystalline or noncrystalline (amorphous) form [3]. Crystalline silica may be found in more than one form: alpha quartz, beta quartz, tridymite, and cristobalite [6]. Three diseases have been associated with exposure to silica dust including silicosis, silicotuberculosis, and cancer [5]. Over the past 20 years, various studies have implicated silica dust as an effective factor in high incidence rate of lung cancer. Therefore, international agency for research on cancer now classifies silica dust as a Group I human carcinogen [1]. An important factor is that the silica dust particles must be small enough to enter the lungs [2]. This size is generally considered to be 10 µm and smaller (PM_{10}). Saffiotti et al. [7] have investigated the mechanisms responsible for the carcinogenic properties of silica dust. For quartz, the PZNPC occurs at a pH of less than 2, and at most pH values the quartz surface is negatively charged and quartz exhibits negative zeta potentials. Trace-metal impurities are attracted to these sites, and an observed reaction was the oxidation of Fe^{2+} to Fe^{3+} [8]. The result is the production of OH^-. Crystalline silica surfaces also produce hydrogen peroxide (H_2O_2) and the hydroxyl radical. The presence of these oxygen free radicals leads to damage and breakage of DNA strands [5].

Kaolin (hydrated aluminum silicate) is a high-value, high-volume industrial clay used largely in the production of paper, as well as ceramics, cement, fiberglass, and many other industrial production processes [6]. Its naturally fine particles mean dust collection is critical in the mining process for air quality improvement and safety [4]. Silica, with an average concentration of more than 46%, is one of the important components of kaolin. Several studies have reported the negative effects of silica dust on the health of miners in kaolin mines [1]. A study was undertaken to determine the dust concentrations in various work areas and to assess the prevalence of radiographic and pulmonary function

* Corresponding author. *E-mail address:* najmeddinali@ut.ac.ir (A. Najmeddin).

abnormalities in 65 workers at a Georgia kaolin mine [9]. The mean respirable dust level in the processing area was 1.74 mg/m^3 and 0.14 mg/m^3 in the mine area. Five workers, all of whom had worked at the processing area, had radiographic evidence of kaolin pneumoconiosis. In this study the highest dust concentrations occurred in the processing area, and kaolin pneumoconiosis was limited to those who had worked there. Kaolin exposure appeared to have a small but significant effect on ventilatory capacity in those with kaolin pneumoconiosis and in workers with a longer exposure.

Many studies have been conducted on the various characteristics of industrial soils; however, a comprehensive study on the environmental effects of mineral dust in these areas has not been conducted [10, 11]. For the first time in Iran, this study investigates the mineralogy, chemical composition, pollution level, and bioaccessibility of potentially toxic elements (PTEs) in kaolin dust of Adalat. The study area lies about 15 km north of Gonabad, where several villages are located close to the mine. Because the suspended particles are extremely fine, they can travel long distances with the wind, raising concerns about their potential impacts on human health. Open-pit mining, mineral crushing, and the movement of mining machinery are the most important sources of particulate matter in the region. In recent years, cases of silicosis have been reported among miners in the region. Therefore, it is necessary to examine the chemical composition and mineralogy of mine dust particles in order to improve their environmental effects in the study area.

2. Materials and methods

2.1. Study area

The study area, Adalat mine, is one of the most important kaolin mines located in South Khorasan Province, eastern Iran. The mine is an active open-pit kaolin extraction site situated within a mineralized zone characterized by intensive mining operations and extensive exposure of fine-grained materials. Two rural settlements, Chahmighuni and Chahnamak, are located in close proximity to the mining area and are potentially affected by dust emissions originating from mining activities. The nearest urban center to the study area is Gonabad City, which represents the main regional population and service center. The selection of this site was motivated by the close spatial relationship between mining activities and nearby residential areas, as well as the high potential for generation, dispersion, and deposition of mineral dust enriched with PTEs. The study area is characterized by a dry to semi-arid climate, typical of eastern Iran, with low annual precipitation, high evaporation rates, and sparse vegetation cover. Precipitation is limited and mainly occurs during the colder months of the year, while prolonged dry periods dominate most of the annual cycle. Such climatic conditions, combined with surface disturbance caused by mining operations, favor the generation and resuspension of mineral dust. The regional wind regime plays a crucial role in the transport and redistribution of airborne particles. Prevailing winds frequently facilitate the horizontal transport of dust from the mining area toward the surrounding environments, including nearby villages.

2.2. Sampling, sample preparation and chemical analysis

To investigate the spatial and temporal variability of PTE contamination, fifty-two dust samples from six stations in Adalat's mine and surrounding areas were collected (Fig. 1). Sampling was taken using passive method in two different seasons. Mineral dust sampling was carried out using a passive sampling approach, which relies on the natural gravitational settling of airborne particles without the use of active air-pumping systems. Passive dust samplers consisting of acid-washed, inert collection surfaces were installed at selected locations around the mine and adjacent residential areas. The sampling devices were exposed for several weeks to months, allowing sufficient accumulation of deposited dust. In the laboratory, dust samples were air-dried or oven-dried at low temperature to remove residual moisture. In general, particles smaller than 80 microns are capable of being suspended in the air [5]. However, in this study, particles smaller than 10 microns in diameter were used to investigate the mineralogical and chemical composition of the particles in the laboratory. These particles are known as respirable particles. Total concentrations of potentially toxic elements were determined following acid digestion using a mixture of strong acids. The resulting solutions were analyzed using ICP-OES. Quality assurance procedures included blanks, duplicates, and certified reference materials.

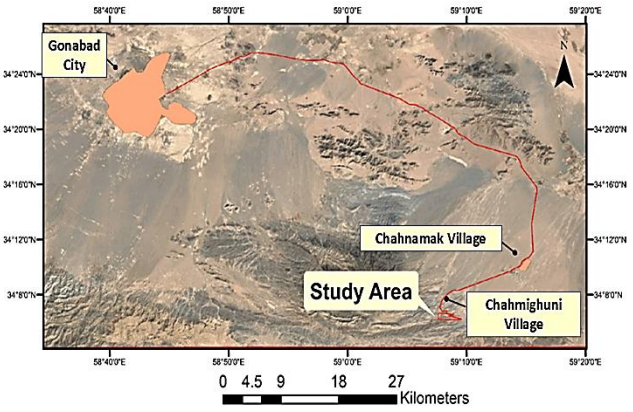

Fig. 1. Map of the study area showing the urban and rural areas.

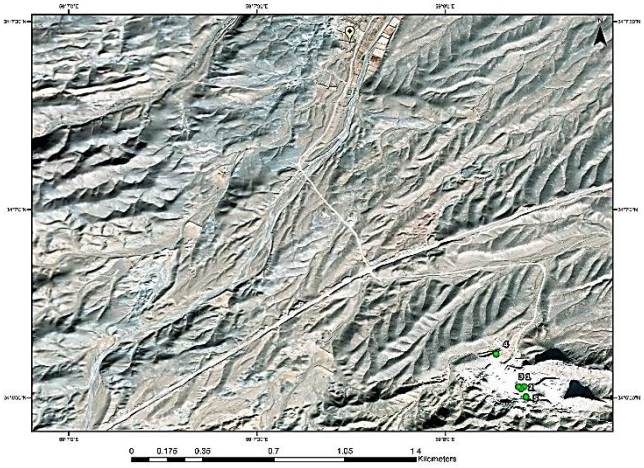

Fig. 2. Sampling stations in the Adalat kaolin mine (five stations) and the Chahmighuni village (one station).

2.3. Pollution assessment

The geo-accumulation index (I_{geo}) proposed by Müller [12] is a widely used contamination index calculated using the following equation:

$$Igeo = \log_2\left(\frac{Cx}{1.5\,Bx}\right) \quad (1)$$

Where C_x is the measured concentration of the element (x) in particulate matter and B_x is the natural background concentration of element (x). Factor 1.5 is used for possible variations in the background data due to lithogenic (natural) effects. This index has seven grades or classes from uncontaminated to extremely contaminated: class 1 (practically uncontaminated/unpolluted), with I_{geo} values less than zero; class 2 (unpolluted to moderately polluted), with I_{geo} values ranging from 0 to 1; class 3 (moderately polluted), with I_{geo} values from 1 to 2; class 4 (moderately to strongly polluted), with I_{geo} values ranging from 2 to 3; class 5 (strongly polluted), with I_{geo} values from 3 to 4; class 6 (strongly to very strongly polluted), with I_{geo} from 4 to 5; and Class 7 (very strongly polluted), with I_{geo} over 5.

2.4. Simple bioavailability extraction test (SBET)

The detailed standard operating procedure of SBET was described in the report of US EPA [13], which is used to investigate the relative bioavailability of PTEs. Briefly, bioavailable PTEs measured using SBET was obtained by extracting 0.5 g of samples with glycine (0.4 M; pH = 1.5 readjusted with concentrated HCl) rotated end-over-end for 1 h at 37 °C. The mixture was centrifuged and the supernatant was filtered through Whatman paper number 42. The pH of the filtrate should be within 0.5 pH units of the starting pH, otherwise the procedure has to be redone. The filtrate samples were stored in a refrigerator at 4 °C until analysis. The extractions were conducted in duplicate. Analysis must be performed within one week after in vitro digestion. In this study, concentrations of PTEs were determined using inductively coupled plasma optical emission spectrometry (ICP-OES, Optima 5300) at the Zarazma laboratory, Iran. La, Nd, Li and Sr were not detected in any sample of the SBET.

2.5. Risk assessment model

A modified version of the United States Environmental Protection Agency (USEPA) model, as adapted by Cao et al. [14], was applied to estimate the health risk posed to adults and children due to exposure to PTEs through ingestion and dermal contact. The non-carcinogenic exposure dose for each PTE and pathway was calculated as:

$$ADD_{ing} = C \times \frac{[IngR \times f] \times [EF \times ED \times 10^{-6}] \times AR}{BW \times AT} \quad (2)$$

$$ADD_{derm} = C \times \frac{[SL \times SA \times f] \times [EF \times ED \times 10^{-6}] \times ABS}{BW \times AT} \quad (3)$$

However, the cancer risk due to exposure to carcinogenic elements (Cr, Pb and Ni) through ingestion was evaluated using the lifetime average daily dose (LADD) following USEPA guidelines [15]:

$$LADD = \frac{C \times EF}{AT \times PEF} \times \left(\frac{IRing_{child} \times ED_{child}}{BW_{child}} + \frac{IRing_{adult} \times ED_{adult}}{BW_{adult}}\right) \quad (4)$$

where ADD_{ing} represents the daily dose from hand-to-mouth ingestion of soil or dust particles, and ADD_{derm} denotes the daily dose from dermal absorption of particles. The ingestion rate (IngR) was assumed as 200 mg/day for children and 100 mg/day for adults [15]. The exposure frequency (EF) was set at 180 days/year [16], the exposure duration (ED) at 6 years for children and 24 years for adults, and the absorption rate (AR) at 0.001 [15]. Exposed skin surface area (SA) values were 1,150 cm² for children and 2,140 cm² for adults [16], while the skin adherence factor (SL) was 0.2 mg/cm²/day for children and 0.7 mg/cm²/day for adults [15]. Dermal absorption factor (ABS) was fixed at 0.001 for all PTEs [16] and the particle emission factor (PEF) at 1.36 × 109 m³/kg [14]. Mean body weights (BW) were assumed as 15 kg for children and 70 kg for adults [13]. The averaging time (AT) was calculated as ED × 365 days for evaluating non-carcinogenic effects through formulas 5-6, and 25,550 days (70 × 365) for assessing carcinogenic effects via formula 7 [16]. In this study, PTE concentrations in the mobile fractions (from the SBET) were used to represent the bioavailable portion. Non-carcinogenic and carcinogenic risks were estimated using:

$$HQ = D/Rfd \quad (5)$$

$$CR = D \times SF \quad (6)$$

Where hazard quotient (HQ) is the ratio of exposure dose (D) to the reference dose (RfD) [15], but hazard index (HI) is the sum of HQ values across all elements and pathways; HI ≤ 1 suggests negligible risk, while HI > 1 indicates potential health effects [16]. Carcinogenic risk (CR) was computed as the product of exposure dose and slope factor (SF) [17].

2.6. Statistical analysis

In linear geostatistics and multivariate statistics, a normal distribution for the data is desirable [18]. In this study, the normality of the data was checked using Shapiro–Wilk test (p > 0.01). The results show that S, As, Pb, and Zn concentrations are non-normally distributed in the kaolin dust samples (significant level < 0.05). Also, values of standardized skewness and kurtosis indicate significant departures from normality that confirmed these elements are not normally distributed. In our study, the Box-Cox transformation was used to make the data more normal and less skewed using SPSS 26 software package. Factor analysis (FA) is a useful statistical tool that can extract latent information from multi-dimensional data and group it into fewer ones [19]. Kaiser–Meyer–Olkin (KMO) and Bartlett's tests were used for the checking of the interest of the implementation of the factor analysis on the data set [18]. In this study, the results of the KMO (0.73) and Bartlett's test (p< 0.001) suggested that factor analysis was suitable for the analysis of the data set. In the present study, FA was performed using the commercial statistics software package SPSS version 26 for Windows.

3. Results and discussion

3.1. Dust mineralogy

The results of X-ray diffractometry indicated that Quartz (SiO_2), Kaolinite ($Al_2Si_2O_5(OH)_4$), Muscovite (and Illite) ($KAl_2Si_3O_{10}(OH)_2$), Jarosite ($KFe_3(SO_4)_2(OH)_6$), and Pyrophyllite ($Al_2Si_4O_{10}(OH)_2$) are dominant minerals in sampling sites (Table 1). Lower abundances of Geothite (FeO(OH)), K-feldspar ($KAlSi_3O_8$), Rutile (TiO_2), Gypsum ($CaSO_4.2H_2O$), Calcite ($CaCO_3$), Alunite ($KAl_3(SO_4)_2(OH)_6$), and Anatase (TiO_2) occur in some samples. According to Salmanzadeh et al. [20], the similarity of mineralogical composition particularly major phases in dust samples indicate that they should have majorly originated from similar sources. The plenty of quartz and calcite in nearly all samples indicates a detrital sedimentary source for the mine dust in the study area. The abundance of quartz is due to resistance to chemical and physical weathering, which allows it to persist over long periods of erosion and transport. The abundance of calcite and clay minerals reflects local geology of the study area [1]. In general, the mineralogy of mine dust is controlled by regional geology and wind direction. Comparison of the mineralogy of dust samples with the geology of study area suggests that geological formations and composition of the soils of surrounding area should have a direct impact on the mineralogical composition and chemistry of the dust samples. Mineralogy of dust samples collected in the nearest village (e.g. Chahmighuni) have some differences with other samples, indicating that dust events also impact the mineralogy and chemistry of dust samples.

Table 1. Gross mineralogy (XRD) of the whole dust samples (%).

Minerals	Minimum	Maximum	Mean	St. Deviation
Major Phases				
Quartz	22	50	41.5	12
Kaolinite	8	28	19	7.5
Muscovite (and Illite)	5	13	9.2	2.8
Jarosite	<1	13	5.3	5.4
Pyrophyllite	<1	34	13.8	14.7
Minor Phases				
Geothite	2	3	2.3	0.5
K-feldspar	2	5	3	1.1
Rutile	<1	3	0.7	1.2
Gypsum	<1	8	3	2.9
Calcite	<1	4	2	1.9
Alunite	<1	13	3.2	5.4
Anatase	<1	3	0.7	1.2

3.2. XRF analysis

The bulk chemical composition of mineral dust collected from the Adalat kaolin mine was determined by X-ray fluorescence (XRF) analysis, focusing on eleven major oxides along with loss on ignition (LOI) (Table 2). Overall, the results indicate a strong consistency between the mineralogical findings obtained XRD analysis and the

geochemical data derived XRF. XRF analysis revealed that the deposited mineral dust is dominated by SiO_2 (59.6 ± 5.6 wt.%) and Al_2O_3 (17.3 ± 2.5 wt.%), reflecting the strong influence of kaolinite-rich source materials. The relatively narrow range of Al_2O_3 (14.6–21.8 wt.%) and elevated LOI values (10.7 ± 1.7 wt.%) further confirm the abundance of hydrous aluminosilicate phases typical of kaolin deposits. Iron oxide concentrations (Fe_2O_3 = 3.23 ± 1.53 wt.%) indicate the presence of iron-bearing accessory minerals or surface coatings, which are known to play an important role in controlling the sorption and transport of potentially toxic elements. Calcium oxide contents are comparatively low (CaO = 2.00 ± 0.95 wt.%), suggesting a limited contribution from carbonate minerals, consistent with the geological setting of the study area.

Alkali oxides (K_2O = 1.51 ± 0.38 wt.%; Na_2O = 0.65 ± 0.30 wt.%) occur in minor amounts and likely originate from feldspar residues and clay-associated phases. Trace oxides such as TiO_2 (0.66 ± 0.19 wt.%), MnO (0.03 ± 0.02 wt.%), and P_2O_5 (0.20 ± 0.09 wt.%) are present at low concentrations, typical of resistant heavy minerals and accessory phases. Elevated SO_3 contents (3.76 ± 2.33 wt.%) in some samples may reflect the contribution of sulfate minerals or secondary atmospheric inputs.

Alkali oxides (K_2O = 1.51 ± 0.38 wt.%; Na_2O = 0.65 ± 0.30 wt.%) occur in minor amounts and likely originate from feldspar remnants and clay-associated phases. Trace oxides such as TiO_2 (0.66 ± 0.19 wt.%), MnO (0.03 ± 0.02 wt.%), and P_2O_5 (0.20 ± 0.09 wt.%) are present at low concentrations, typical of resistant heavy minerals and accessory phases. Elevated SO_3 contents (3.76 ± 2.33 wt.%) in some samples may reflect the contribution of sulfate minerals or secondary atmospheric inputs.

Table 2. Major oxide composition (wt.%) of mine dust. Values are reported as mean ± standard deviation (SD) together with minimum and maximum concentrations.

Oxide	Mean ± SD	Minimum–Maximum
SiO_2	59.58 ± 5.57	52.05–68.03
Al_2O_3	17.33 ± 2.45	14.63–21.83
Fe_2O_3	3.23 ± 1.53	1.46–5.46
CaO	2.00 ± 0.95	0.77–3.08
K_2O	1.51 ± 0.38	1.18–2.20
Na_2O	0.65 ± 0.30	0.29–1.06
MgO	0.16 ± 0.10	0.01–0.28
TiO_2	0.66 ± 0.19	0.42–0.96
MnO	0.03 ± 0.02	0.007–0.064
P_2O_5	0.20 ± 0.09	0.066–0.32
SO_3	3.76 ± 2.33	0.26–6.68
LOI	10.72 ± 1.72	8.99–13.62

3.3. Comparison with global mineral dust

When compared with globally reported mineral dust compositions, the dust from the Adalat kaolin mine shows both similarities and distinctive features. Average Saharan dust typically contains SiO_2 ~60–65 wt.%, Al_2O_3 ~15–18 wt.%, and CaO ~5–10 wt.%, reflecting a stronger carbonate influence [6]. In contrast, Asian desert dust generally exhibits SiO_2 ~55–65 wt.%, Al_2O_3 ~14–17 wt.%, and CaO ~3–7 wt.% [2]. The studied dust closely matches global dust in terms of SiO_2 and Al_2O_3 but shows markedly lower CaO and higher LOI, indicating a clay-rich, carbonate-poor source dominated by kaolin lithologies. This compositional signature distinguishes the Adalat dust from typical carbonate-influenced arid-region dust and suggests reduced buffering capacity against acidic inputs, potentially enhancing the mobility of toxic elements upon deposition.

The combination of high Al_2O_3, elevated LOI, and fine-grained clay-rich composition suggests a high specific surface area and strong adsorption capacity for trace metals. Consequently, the mineral dust in the vicinity of the Adalat kaolin mine may act as an efficient carrier of potentially toxic elements, increasing their environmental persistence and potential exposure risks for nearby rural settlements.

3.4. PTEs concentrations in mine dust

Descriptive statistical analysis of PTEs in mine dust collected from the Adalat kaolin mine (Table 3) reveals pronounced variability in elemental concentrations, reflecting heterogeneous source contributions and complex geochemical controls. The wide ranges observed between minimum and maximum values for several elements indicate substantial spatial variability within the study area, likely driven by differences in lithology, mining intensity, and localized dust generation processes. Major lithogenic elements such as Al (62,634–88,500 mg/kg) and Fe (6,952–28,175 mg/kg) exhibit relatively stable distributions, as evidenced by the close agreement between mean and median values and low skewness coefficients (−0.13 and 0.84, respectively). These features suggest predominantly crustal control and limited influence of localized enrichment processes. Correspondingly, their coefficients of variation (CV < 50%) indicate moderate variability and a relatively uniform background contribution from clay-rich and iron-bearing minerals. In contrast, trace and potentially toxic elements including As, Cu, Pb, Zn, Li, and Mg display markedly higher dispersion, reflected by large standard deviations and elevated CV values. Particularly high CVs for Pb (118.25%), Zn (99.56%), Mg (82.86%), and Li (65.11%) indicate strong heterogeneity and the presence of concentration hotspots. Such variability is commonly associated with anthropogenic disturbances, selective mineral enrichment, or localized accumulation of fine particles capable of retaining trace elements.

The positive skewness observed for most PTEs (e.g., Pb = 1.95, Cu = 1.25, Zn = 1.28) indicates right-skewed distributions, implying that while most samples exhibit moderate concentrations, a limited number contain substantially elevated values (Table 3). This pattern is characteristic of mining-impacted environments and suggests episodic or point-source inputs superimposed on a regional geochemical background. High kurtosis values for Pb (5.01), Cu (2.67), and Zn (2.05) further support the presence of peaked distributions with extreme values, highlighting the potential environmental relevance of these elements despite relatively low median concentrations. Elements such as Sr and Nd show comparatively low skewness and kurtosis, along with moderate CV values, suggesting a more homogeneous spatial distribution governed largely by mineralogical composition rather than external inputs. Sulfur (S) exhibits substantial variability (CV = 60.11%), likely reflecting the combined influence of sulfate-bearing minerals, atmospheric deposition, and mining-related emissions.

Geoaccumulation index (I_{geo}) is used to assess the degree of dust contamination by PTEs. In this study, elemental contents in world soils [21, 22] were used as background values for calculating I_{geo}. The results indicated as boxplots in Fig. 3. Results indicate various degrees of enrichment above the background, ranging from uncontaminated to strongly polluted (Fig. 3). The median I_{geo} values decreased in the following order: As > S > Sr >> Al = Li = La = Nd = Cu = Pb = Fe = Mg = Zn. It is obvious that I_{geo} variations are greater in the first three elements. Also, Igeo values for Pb variates from -5.6 (unpolluted) to 1.5 (moderately polluted). The I_{geo} values for As, S, Sr, Li and Pb are substantially higher than for other elements.

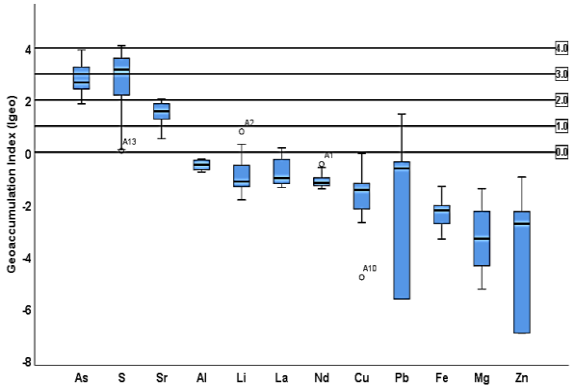

Fig. 3. Summary of the results of Igeo for mine dust samples.

Table 3. Descriptive statistics of PTEs concentration in dust samples.

Element	Minimum	Maximum	Mean	Standard deviation	Median	Skewness	Kurtosis	CV(%)
Al	62634	88500	75927	10102.25	75848	-0.13	-1.84	13.31
As	25.6	107	53.82	23.12	45.1	1.07	0.78	42.96
Cu	0.75	20.4	7.85	4.94	7.66	1.25	2.67	62.93
Fe	6952	28175	15410.46	6980.68	14918	0.84	-0.34	45.3
Ga	10.2	26.8	16.93	5.37	14.2	0.65	-0.92	31.72
La	17.5	50.4	27.29	10.65	22.5	1.09	0.07	39.03
Li	32.8	203	79.16	51.54	53.4	1.43	1.49	65.11
Mg	215	3130	1096.54	908.61	826	1.14	0.45	82.86
Nd	18.6	36	24.25	5.75	21.9	1.13	-0.02	23.71
Pb	0.75	103	23.83	28.18	24.3	1.95	5.01	118.25
S	1280	21039	10756.85	6465.41	11140	0.07	-0.94	60.11
Sr	536	1557	1106.15	307.51	1116	-0.24	-0.88	27.8
Zn	0.75	47.9	13.74	13.68	13.8	1.28	2.05	99.56

Inter-element relationships can provide considerable information on PTE sources and pathways [23]. In this study, FA was applied to classify the studied PTEs in mine dust of Adalat by applying varimax rotation with Kaiser normalization. The number of significant factors and the percent of variance were calculated by extracting the values and eigenvalues from the correlation matrix. The results of FA are presented in Table 4 and Fig. 3.

The FA results identified three factors with eigenvalues greater than unity, collectively accounting for 74.6% of the total variance, indicating a robust explanation of the geochemical variability within the dataset. Factor 1 (F1) explains 33% of the total variance and is characterized by strong loadings of Li, Sr, Al, and Zn. Considering the XRD results and the spatial consistency in the concentration patterns of these elements across the study area, F1 is interpreted as representing a lithogenic source associated with aluminosilicate minerals, particularly kaolinite, which constitutes the dominant clay phase of the Adalat kaolin mine. The relatively uniform spatial distribution of these elements further supports their terrigenous origin, reflecting the natural geochemical background of the host material.

Factor 2 (F2) accounts for 24.5% of the total variance and is predominantly influenced by La, Mg, Nd, and S. Notably, the concentrations of these elements are substantially higher in samples collected from the mining zone compared to those from surrounding rural areas. This spatial enrichment suggests a source linked to mineralogical heterogeneity within the mining area, likely associated with the presence of accessory and minor phases enriched in rare earth elements (REEs). The contribution of F2 therefore reflects a mixed geogenic signature, controlled by localized mineral assemblages exposed or concentrated through mining activities.

Factor 3 (F3), explaining 17.3% of the total variance, is primarily loaded by Cu, Fe, Pb, and As. The co-association of these elements, particularly those recognized for their environmental and toxicological significance, indicates an anthropogenic influence. This factor is interpreted as reflecting local human-induced inputs, potentially arising from mining operations, machinery emissions, and the mobilization of iron oxides that serve as effective carriers for potentially toxic elements. The enrichment of Cu, Pb, and As in association with Fe suggests that iron-bearing phases play a key role in concentrating and transporting these contaminants within the dust matrix.

Overall, the FA results highlight a clear differentiation between natural lithogenic contributions and anthropogenic inputs, providing critical insight into the controlling mechanisms governing PTEs distribution in mineral dust from the Adalat kaolin mine. This distinction is essential for accurately interpreting environmental behavior and for subsequent health risk assessments in the region.

3.5. Bioaccessibility of elements in mine dust

The results of the SBET provide valuable insight into the fraction of PTEs in mine dust that can become available for absorption through the ingestion exposure pathway [18]. In this study, bioaccessibility was quantified as the percentage of each element extracted by SBET relative to its total concentration in the dust samples (Fig. 5), thereby reflecting the potential mobility of elements under simulated gastrointestinal conditions. Among the analyzed elements, As, Pb, Fe, Mg, and S exhibited comparatively higher bioaccessibility, with arsenic showing the highest mean bioaccessible fraction (73.1%). Such a high bioaccessible proportion of As is particularly noteworthy, as it indicates that a substantial fraction of total arsenic in the dust is readily soluble under gastric conditions and therefore potentially available for systemic uptake following ingestion. The SBET results reveal the following order based on mean values: As > Fe > Pb > S > Mg ≈ Al ≈ Cu ≈ Zn, suggesting that there were great differences of element bioaccessibility among these studied elements. The observed differences in bioaccessibility can be largely attributed to element-specific geochemical behavior and mineralogical associations. Arsenic and lead are commonly associated with surface-bound phases such as iron oxides and poorly crystalline mineral coatings, which tend to dissolve under acidic gastric conditions, thereby enhancing their bioaccessible fractions. Similarly, the relatively high bioaccessibility of Fe and S suggests the presence of reactive iron-bearing minerals and sulfate phases that are susceptible to dissolution in the SBET solution. In contrast, elements such as Al, Cu, and Zn, which are more strongly incorporated into stable aluminosilicate lattices or less reactive mineral phases, exhibited comparatively lower bioaccessibility. Spatially, the highest SBET values for As, Fe, S, and Pb were consistently observed in samples collected from the mining area, indicating that mining activities likely enhance the formation or exposure of more reactive mineral phases. Mechanical disturbance, crushing, and increased surface area of particles in the mine environment can promote the enrichment of labile metal-bearing phases, thereby increasing their solubility under simulated gastrointestinal conditions. This finding underscores the role of mining operations not only in elevating total metal concentrations, but also in modifying their chemical forms toward more bioaccessible and potentially harmful states.

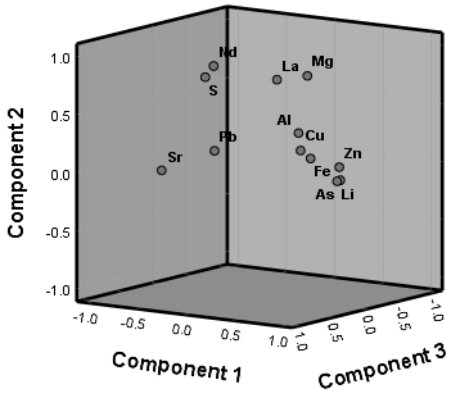

Fig. 4. Component plot in rotated space for studied PTEs in mine dust.

Table 4. Principal component loadings, eigenvalues, % of variance and communalities of PTEs in mine dust.

Elements	Factor 1	Factor 2	Factor 3	Communalities (extraction)
Al	0.695	0.424	0.418	0.838
As	0.028	-0.023	0.854	0.730
Cu	-0.117	0.019	-0.773	0.612
Fe	0.191	0.024	-0.481	0.268
La	0.368	0.829	0.269	0.895
Li	0.936	0.000	0.192	0.913
Mg	0.316	0.782	-0.255	0.776
Nd	-0.286	0.881	0.269	0.931
Pb	0.023	0.243	0.699	0.548
S	-0.590	0.709	-0.041	0.853
Sr	-0.797	-0.065	0.306	0.734
Zn	0.609	0.017	-0.307	0.465
Total Eigenvalues	3.874	3.116	1.683	-
Percentage of Variance	32.753	24.528	17.271	-
Cumulative Variance (%)	32.753	57.281	74.552	-

From a human health perspective, the elevated bioaccessibility of toxic elements, particularly As and Pb, implies that risk assessments based solely on total concentrations may underestimate actual exposure levels. The SBET results therefore provide critical input for more realistic health risk assessments, especially for populations residing near the mine who may be exposed to dust through incidental ingestion. Overall, the bioaccessibility patterns observed in this study emphasize the importance of considering both total elemental content and bioaccessible fractions when evaluating the environmental and health implications of mineral dust in mining-impacted areas.

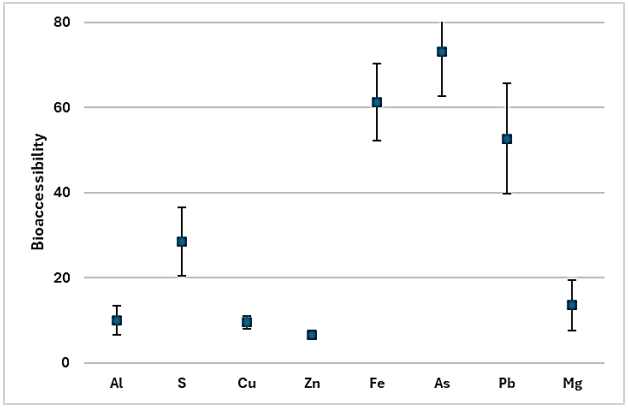

Fig. 5. Bioaccessibility (i.e. the percentage of SBET-extractable content to total content) of PTEs in the dust samples.

3.6. Human health risk assessment model

The exposure doses of toxic elements associated with mine dust from the Adalat kaolin mine were estimated for both children and adults, and the corresponding hazard quotients (HQs) for different exposure pathways, along with hazard indices (HIs), are summarized in Table 5. Overall, the results indicate that non-carcinogenic health risks are consistently higher for children than for adults, reflecting the greater vulnerability of children due to lower body weight, higher dust ingestion rates, and more frequent hand-to-mouth activities. Quantitatively, the HQ values for children via the ingestion pathway were on average 1.3 to 6.8 times higher than those calculated for adults, clearly identifying ingestion as the dominant exposure route for both age groups. This finding is consistent with the physicochemical characteristics of the dust, particularly its fine particle size and elevated bioaccessible fractions of toxic elements such as As and Pb, as demonstrated by the SBET results. Inhalation constituted the second most important exposure pathway, whereas dermal contact contributed negligibly to overall risk.

When considering non-carcinogenic effects for children, the calculated HI values decreased in the following order: As > S > Pb > Fe > Sr > Mg > Li > Cu > La > Zn > Al > Nd. These ranking highlights arsenic as the most critical contributor to potential health risk, which is consistent with its high total concentration, strong association with reactive mineral phases, and exceptionally high bioaccessibility observed in the mine dust. For both children and adults, As exhibited the highest HI value (0.118), whereas Al showed the lowest (0.000178), reflecting its relatively low toxicity and limited bioaccessible fraction despite its high total abundance. Importantly, although HI values for all studied elements remained below the widely accepted safety threshold of 1, indicating no immediate non-carcinogenic risk, these results should be interpreted with caution in the context of mining environments. The cumulative exposure to multiple toxic elements, particularly As, Pb, and Cu, combined with chronic exposure frequency and enhanced bioaccessibility, may still pose long-term health concerns for populations residing near the mine. Such cumulative and synergistic effects are not fully captured by single-element HI values and warrant careful consideration in environmental management strategies.

The carcinogenic risk associated with arsenic exposure was evaluated through the ingestion pathway, as this route contributed most significantly to total exposure. The calculated carcinogenic risk (CR) for As was 4.13×10^{-8}, which is well below the internationally accepted precautionary threshold of 10^{-6} [24]. This result suggests that the carcinogenic risk posed by arsenic in superficial mine dust is currently within acceptable limits. Nevertheless, given the persistence of arsenic in the environment and its high bioaccessibility, continued monitoring and exposure mitigation measures are strongly recommended.

Overall, the health risk assessment results, when interpreted alongside the mineralogical composition, factor analysis, and bioaccessibility data, indicate that while immediate health risks are limited, the mine dust represents a potential long-term concern, particularly for children, due to repeated exposure to bioaccessible toxic elements.

4. Conclusions

This study provides a comprehensive assessment of mineral dust generated from the Adalat kaolin mine by integrating bulk geochemistry, multivariate statistical analysis, bioaccessibility, and human health risk evaluation. The main mineralogical drivers (silicates) and key contaminant elements identified. The XRF results revealed that the dust is dominated by aluminosilicate components, reflecting the kaolinitic nature of the host material, while notable spatial variability was observed for several PTEs. Factor analysis successfully distinguished between lithogenic sources associated with aluminosilicate minerals and localized mineralogical heterogeneity, as well as an anthropogenic

Table 5. Non-carcinogenic and carcinogenic health risk indices associated with exposure to toxic elements in mine dust.

Element	Dominant Exposure Pathway	HI (Children)	HI (Adults)	Non-carcinogenic Risk Level	Carcinogenic Risk (CR)	Risk Interpretation
As	Ingestion	0.118	< 0.118	Below threshold (HI < 1)	4.13×10^{-8}	Acceptable
S	Ingestion	< 1	< 1	Acceptable	-	Non-carcinogenic only
Pb	Ingestion	< 1	< 1	Acceptable	-	Potential cumulative concern
Fe	Ingestion / Inhalation	< 1	< 1	Acceptable	-	Low risk
Sr	Ingestion	< 1	< 1	Acceptable	-	Low risk
Mg	Ingestion	< 1	< 1	Acceptable	-	Low risk
Li	Ingestion	< 1	< 1	Acceptable	-	Low risk
Cu	Ingestion	< 1	< 1	Acceptable	-	Potential cumulative concern
La	Ingestion	< 1	< 1	Acceptable	-	Low risk
Zn	Ingestion	< 1	< 1	Acceptable	-	Low risk
Al	Ingestion	0.000178	< 0.000178	Negligible	-	Minimal risk
Nd	Ingestion	< 1	< 1	Acceptable	-	Low risk

component characterized by toxic elements such as As, Pb, Cu, and Fe. Bioaccessibility results highlighted substantial differences among elements, with arsenic exhibiting particularly high bioaccessible fractions under simulated gastric conditions. This finding underscores the importance of considering chemical speciation and mineral associations, rather than relying solely on total concentrations, when evaluating potential exposure risks. Overall, the results demonstrate that while overall hazard indices are below the threshold, arsenic is the predominant risk contributor due to its high concentration and high bioaccessibility. The core implication is that dust from these mining areas, particularly due to bioaccessible arsenic, poses a measurable and ongoing health risk that warrants management attention, despite not exceeding the current safety threshold. The integrated approach adopted in this study provides a robust framework for evaluating environmental and health implications of mineral dust in mining regions and can be applied to similar settings worldwide.

Acknowledgement

The authors wish to express their gratitude to the Sepidkavan company and research committee of Ferdowsi University of Mashhad for logistic help.

Conflict of interest:

The authors declare that they have no conflict of interest.

References

[1]. Yu, H., & Zahidi, I. (2023). Environmental hazards posed by mine dust, and monitoring method of mine dust pollution using remote sensing technologies: An overview. Science of the Total Environment 864: 161135. http://dx.doi.org/10.1016/j.scitotenv.2022.161135.

[2]. Mostafa, M., Farhat, H., Abd El-Bakey, S., Zakaria, M., Zekry, H., & Abu Elwafa, R. (2025). Release of potentially toxic elements from an operational phosphate mine (Sebaiya east, Egypt): geochemical characterizations, environmental risks and mining sustainability. Journal of Environmental Earth Sciences 84:445. https://doi.org/10.1007/s12665-025-12448-1.

[3]. Wang, Zh., Zhou, W., Jiskani, I. M., Luo, H., Ao, Zh., Mvula, E. M. (2022). Annual dust pollution characteristics and its prevention and control for environmental protection in surface mines. Science of the Total Environment 825:153949. http://dx.doi.org/10.1016/j.scitotenv.2022.153949.

[4]. Abbasi, S., Hashemi, N., Rahnama, Sh., Najmeddin, A., Yousefi, M. R., Kardel, F. et al. (2025). Regional and climatic variations in atmospheric microplastic deposition: A study throughout Iran. Environmental Technology & Innovation 40: 104577. https://doi.org/10.1016/j.eti.2025.104577.

[5]. Eby, G.N. (2004). Principles of Environmental Geochemistry. Waveland Press.

[6]. Dill, H. G. (2016). Kaolin: Soil, rock and ore From the mineral to the magmatic, sedimentary and metamorphic environments. Earth-Science Reviews 161: 16–129. http://dx.doi.org/10.1016/j.earscirev.2016.07.003.

[7]. Saffiotti, U., Daniel, L. N., Mao, Y., Williams, A. 0., Kaighn, M. E., Ahmed, N., & Knapton, A. D. (1993). Biological studies on the carcinogenic mechanisms of quartz. In Guthrie, G. D., Jr., and Mossman, B. T. (eds.). Health Effects of Mineral Dusts Reviews in Mineralogy, v. 28. Washington, DC: Mineralogical Society of America, pp. 523-544.

[8]. Ishtiaq, M., Jehan, N., Akbar Khan, S., Muhammad, S., Saddique, U., Iftikhar, B., & et al. (2018). Potential harmful elements in coal dust and human health risk assessment near the mining areas in Cherat, Pakistan. https://doi.org/10.1007/s11356-018-1655-5.

[9]. Wu, L., & Song, Z. (2022). Dust pollution characteristics and control measures of open cut coal mines. Scientific Mining Journal 3: 131 – 140. https://doi.org/1030797/madencilik.1149989.

[10]. Sarkheil, H., Shahbaznejad, M., Rayegani, B., Mohtat, Y., Salahjou, T., & Sadeghy Nejad, A. (2025). Lithium extraction assessment from brines in Kerman province: challenges and opportunities for clean energy transition and climate change mitigation. International journal of mining and geo-engineering, 59(3): 191-200.

[11]. Sarkheil, H., Sadeghy Nejad, A. & Rostamian, E. (2025). Climate-smart mining through block matrix analysis: a conceptual modeling approach for sustainable resource governance. International journal of mining and geo-engineering. Articles in Press.

[12]. Muller, G. (1969). Index of geoaccumulation in sediments of the Rhine River. Geojournal, 2, 108-118.

[13]. U.S. Environmental Protection Agency (EPA). (2008). Standard Operating Procedure for an In Vitro Bioaccessibility Assay for Lead in Soil EPA 9200. pp. 1–86.

[14]. Cao, Z., Zhao, L., Zhu, G., Chen, Q., Yan, G., Zhang, X., & et al. (2017). Propositional modification for the USEPA models for human exposure assessment on chemicals in settled dust or soil. Environ Sci Pollut Res 24(24): 20113–20116.

[15]. U.S. Environmental Protection Agency (EPA). (2001). Risk

assessment guidance for superfund: volume III -part A, process for conducting probabilistic risk assessment. EPA 540-R-02-002.

[16]. Ferreira-Baptista, L., De Miguel, E. (2005). Geochemistry and risk assessment of street dust in Luanda, Angola: a tropical urban environment. Atmos Environ 39:4501–4512.

[17]. Zhang, J., Deng, H., Wang, D., Chen, Z., & Xu, S. (2013). Toxic heavy metal contamination and risk assessment of street dust in small towns of Shanghai suburban area, China. Environ Sci Pollut Res 20:323–332. https://doi.org/10.1007/s11356-012-0908-y.

[18]. Najmeddin, A., Moore, F., Keshavarzi, B., & Sadegh, Z. (2018). Pollution, source apportionment and health risk of potentially toxic elements (PTEs) and polycyclic aromatic hydrocarbons (PAHs) in urban street dust of Mashhad, the second largest city of Iran. J. Geochem. Explor. 190, 154–169. https://doi.org/10.1016/j.gexplo.2018.03.004.

[19]. Keshavarzi, B., Tazarvi, Z., Rajabzadeh, M. A., & Najmeddin, A. (2015). Chemical speciation, human health risk assessment and pollution level of selected heavy metals in urban street dust of Shiraz, Iran. Atmospheric Environment,119, 1–10. doi:10.1016/j.atmosenv.2015.08.001.

[20]. Salmanzadeh, M., Saeedi, M., Li, L.Y., Nabi-Bidhendi, Gh. (2015). Characterization and metals fractionation of street dust samples from Tehran, Iran. Int. J. Environ. Res. 9(1), 213–224.

[21]. Alloway, B. (2010). Heavy Metals in Soils: Trace Metals and Metalloids in Soils and their Bioavailability, third ed. Springer Publications, p. 614.

[22]. Liu, E., Yan, T., Birch, G., Zhu, Y. (2014). Pollution and health risk of potentially toxic metals in urban road dust in Nanjing, a mega-city of China. Sci. Total Environ. 476, 522–531.

[23]. Nematollahi, M.J., Abbasi, S., Mohammadi, Z., Najmeddin, A., Moravej, S., Yousefi, M.R., & et al. (2022). Evaluation of the 13 May 2018 frontal dust storm in Shiraz: Stable isotopes signature, source apportionment, and concentration of potentially toxic elements. Aeolian Research 58: 100820. https://doi.org/10.1016/j.aeolia.2022.100820.

[24]. Wang, X.S., Qin, Y., & Chen, Y.K. (2007). Leaching characteristics of arsenic and heavy metals in urban roadside soils using a simple bioavailability extraction test. Environ. Monit. Assess. 129, 221–226